Surfactant and Plasticiser Segregation in Thin Polyvinyl Alcohol Films

Arron Briddick[1], Peixun Li[2], Arwel Hughes[2], Florence Courchay[3], Alberto Martinez[3] and Richard L. Thompson[1,*]

[1] Department of Chemistry, Durham University, Science Site, Durham DH1 3LE, U.K.

[2]STFC ISIS Facility, Rutherford Appleton Laboratories, Chilton, Didcot, OX11 0QX, U.K.

[3]Procter&Gamble, Brussels Innovation Center (BIC), Temselaan 100, 1853 Strombeek Bever, Brussels, Belgium

ABSTRACT: The vertical depth distribution of individual additive components (cetyltrimethylammonium bromide (CTAB) and deuterated pentaethylene glycol monododecyl ether (d_{25}-$C_{12}E_5$) and deuterated glycerol (d-glycerol) in PVA film have been isolated and explored by ion beam analysis techniques and neutron reflectometry. The additives display an unexpectedly rich variety of surface and interfacial behaviour in spin-cast films. In separate binary films with PVA, both d-glycerol and CTAB were evenly distributed, whereas d_{25}-$C_{12}E_5$ showed clear evidence for surface and interfacial segregation. The behaviour of each surfactant in PVA was reversed when the plasticiser (glycerol) was also incorporated into the films. With increasing plasticiser content, the surface activity of d_{25}-$C_{12}E_5$ systematically decreased, but remarkably when glycerol and CTAB were present in PVA, the surface and interfacial activity of CTAB is dramatically increased by the presence of glycerol. Quantification of the surface excess by ion beam analysis reveals that in many cases the adsorbed quantity far exceeds what could reasonably be accounted for by a single layer; therefore indicates a wetting transition of the small molecules at the surface or interface of the film. It appears that the surface and interfacial behaviour is partly driven by the relative surface energies of the components, but is also significantly augmented by the incompatibility of the components.

INTRODUCTION

Poly (vinyl alcohol) (PVA) is a semi-crystalline synthetic polymer with excellent film forming ability and optical transparency. PVA is used primarily in the food packaging, medical and now increasingly in the laundry industry due to its resistance to organic solvents, aqueous solubility, biodegradability and low environmental impact. The food packaging industry has used PVA to prolong the lifetime of stored foods without contamination,[1] and there are many medical applications including both implantable and non-implant devices.[2-5] PVA's primary use in the laundry industry is the encapsulation of detergent for unit dose clothes washing. While neat and plasticised PVA have been studied extensively, relatively little attention has been devoted to the surface properties of thin PVA films.

PVA cannot be synthesised directly from vinyl alcohol, but is instead prepared by the hydrolysis of poly (vinyl acetate) (PVAc), and so is typically a copolymer of PVA with some residual PVAc. The degree of hydrolysis (DH) is a measure of the percentage of $-OC(=O)CH_3$ acetate groups that have been converted to -OH groups in the final polymer, and the number and position of residual acetate groups largely determines the properties of the polymer, having the most significant effect on water solubility. Resins with lower DH (< 95%) show a significant increase in solubility because crystallinity is decreased by the presence of more hydrophobic acetate groups, which disrupt the stereoregularity of the polymer chain and do not readily participate in intra/intermolecular H-bonding.[6] Degree of polymerisation has also shown to be correlated to water-solubility, with lower molecular weight PVA chains showing greater solubility at ambient temperatures.[7] However desirable mechanical properties such as tensile strength are also reduced at

lower molecular weight[8], so these characteristics of the resin must be tailored to the application. Although the properties of pure PVA films are extensively customisable through altering these parameters, PVA alone is still generally too brittle and inflexible for many uses.

Plasticizers can be introduced to improve film flexibility whilst maintaining relatively good mechanical properties (tensile, shear strength). In PVA, plasticiser collects in the amorphous regions of the polymer, causing an increase in free volume and a lowering of glass transition temperature (T_g). Glycerol is commonly used to plasticize PVA due to its low molecular weight, low volatility and good compatibility with the host polymer.[9] A truly compatible plasticiser should exhibit homogenous distribution throughout the host polymer matrix, hence mapping of the glycerol locale within PVA can be used to characterize the nature of plasticization. Plasticized films used in industry come in to contact with a number of compounds and environments depending on their intended use, and long-term product stability may be compromised by migration and adsorption of plasticisers in or out of the PVA matrix. Our interest is in determining how small molecules such as surfactants and plasticisers are distributed in simple mixtures with PVA, and how this behaviour is altered by the complexity of multiple components.

Mixtures of polymers and small molecules are widely applied in plasticised materials for packaging, adhesives and coatings, and their use in complex formulations is well characterised, but usually only on an empirical level. There remains a fundamental science challenge in predicting the behaviour of all but the simplest model systems, as the interplay between different components involves complex interactions between ionic, polar and nonpolar groups and phenomena arising from these interactions span length scales ranging from atomistic to several microns. The presence of surfaces or interfaces further complicates this situation, although it is at least possible to rationalise the key factors responsible for the preferential segregation of one component over another at an interface. Firstly the component with the lowest surface energy should be enriched at the surface of a mixture. In the absence of any discernible difference in surface energy, it has been shown that molecular size is significant, with the lower molecular weight component, being enriched at the surface.[10] The extent of surface segregation is further augmented by reducing the compatibility of the components. In surfactant solutions it is well known that increasing the hydrocarbon chain length of a surfactant in an aqueous solution reduces the equilibrium surface tension by promoting adsorption at lower concentrations.[11] In polymer blends increasing incompatibility (increasing Flory Huggins interaction parameter) enhances surface segregation, and ultimately leads to the formation of a wetting layer.[12]

Although the surface adsorption of surfactants and polymers in solutions is a mature area of research, the reverse case where the solvent is replaced by a high molecular weight polymer has received less attention. Of particular relevance to our present work is that of Edler *et al* concerning film forming polymers and surfactants. Here it has been noted that significant interactions between ionic groups of cationic surfactants and lone pairs of water soluble polymer, notably poly(ethyleneimine), "PEI",can lead to the formation of complexed films.[13-14] The fact that film formation is spontaneous indicates that surfactant polymer interactions may have quite dramatic effects on the properties of polymer films, which is the focus of our work. Here we explore for the first time the surface and interfacial segregation of two model surfactants and a plasticiser in PVA film. The ion beam analysis and neutron reflection techniques that we have used enable the depth distribution of a single component within a complex mixed film to be isolated. In addition to simple binary polymer + surfactant or plasticiser mixtures, we also consider the more complex and (industrially relevant) situation of surfactant and plasticiser in a PVA film. Commercial formulations of PVA film interact with plasticizers and surfactants when used in several products; therefore the distribution of these components is very relevant to the bulk and surface properties of these materials. Our results show that even simple models for complex industrial formulations, a surprisingly rich variety of behaviour can result from their interactions.

EXPERIMENTAL

Materials and sample preparation.

PVA resin (Sigma-Aldrich P8136, M_w = 30-70 kg/mol, degree of hydrolysis (DH) = 87-90%), glycerol (Aldrich), d5-glycerol (CK isotopes), CTAB (Acros Organics, 99+%) were purchased and used as received. Pentaethylene glycol deuterated monododecyl ether (d_{25}-$C_{12}E_5$) was prepared at Rutherford Appleton Laboratories according to the method described elsewhere.[15-16]

Aqueous 4 w/v% PVA solutions were prepared in de-ionized water, by heating to 75 °C and stirring until the resin had completely dissolved. Aqueous solutions of the small molecules: glycerol, d5-glycerol, CTAB and d_{25}-$C_{12}E_5$ were also made at 4% (w/v). Polymer + surfactant and/or glycerol solutions

were then prepared from these stock solutions in defined mass ratios and thoroughly mixed to yield 4% (w/v) solutions from which films could be cast. Films of between 150 and 300 nm thickness were prepared by spin-coating the mixed solutions onto fresh silicon wafers. Prior to coating, the silicon wafers were cleaned with acetone to remove any traces of hydrophobic impurities and ensure consistent film production.

Ion beam analysis.

Vertical concentration profiles of components within the spin-cast films by the ion beam analysis techniques of Rutherford backscattering spectroscopy (RBS) and nuclear reaction analysis (NRA), using a National Electrostatics Corporation 5SDH Pelletron Accelerator with RC43 endstation. The application of ion beam analysis techniques to soft matter are described in greater detail elsewhere.[17-18] During these experiments, sample integrity was maintained by cooling to below -50 °C using a liquid-nitrogen cooled sample holder. As well as minimising sample degradation due beam damage, this step was essential to retain the low molecular weight components in the films under the vacuum (< 4×10^{-6} Torr). Due to the low film thickness and macroscopic surface area, glycerol and non-ionic surfactant evaporation under ambient conditions were detectable over a period of hours, so films for ion beam analysis were vitrified by submerging the sample in liquid nitrogen immediately prior to ion beam analysis experiments.

RBS experiments were carried out using a 1.5 MeV $^4He^+$ ion beam incident on the sample surface at 80° degrees to the sample normal. The energy of backscattered $^4He^+$ ions was determined using Canberra PIPS detector with nominal energy resolution of 17 keV at 170° to the incident beam in Cornell geometry. The same detector setup was used for NRA experiments, except in this case, a 700 keV $^3He^+$ ion beam was incident on the samples.

RBS is particularly well suited to quantifying the vertical concentration profile of heavy elements in a matrix of lighter elements. In these experiments, the cationic surfactant, cetyl-trimethylammonium bromide (CTAB) was chosen as a model ionic surfactant. The bromide ion of each CTAB molecule is by far the heaviest element present in the sample; therefore is sensitively resolved by RBS. The absence of any other ionic species within the CTAB / PVA films coupled with the requirement of charge neutrality ensures that the Br- ion depth distribution is representative of the CTAB distribution as a whole. Under these experimental conditions, RBS provides a depth resolution of ~15 nm.

The other two species of interest, glycerol and a non-ionic surfactant contain no elements that distinguish them from the PVA matrix, so their deuterium labelled analogues were used as model materials. Deuterium labelling enables the depth distributions of these molecules in PVA to be quantified by nuclear reaction analysis (NRA) or neutron reflectometry (NR), while having a minimal impact on their physic-chemical properties. NRA experiments were carried out on samples containing deuterium labelled glycerol and deuterium labelled non-ionic surfactant (d_{25}-$C_{12}hE_5$). The glycerol was 1,1,2,3,3-d5 glycerol, chosen so that only non-labile C-D hydrogens of the molecule were deuterated, but the hydroxyl groups were not. (Isotope exchange between labile OH and OD bonds must be avoided to maintain the ability to resolve the small molecules from the polymers.) For these experiments, samples were irradiated with a beam of 0.7 MeV $^3He^+$ ions at 80° to the sample normal. The energy of the backscattered protons resulting from the reaction between ^3He and ^2H within the polymer was analysed to determine the composition versus depth profile of the deuterated component. Under these experimental conditions, NRA provides a depth resolution of ~8 nm, which, similarly to RBS is large compared to the molecular dimensions, but sufficient to quantify adsorption of these components at exposed surfaces or buried interfaces. All IBA data were analysed with the Surrey University DataFurnace[19] software (WiNDF v9.3.68 running NDF v9.6a) to determine the concentration versus depth profile, where the densities of PVA and glycerol were assumed to be 1.19 g/cm^3 and 1.26 g/cm^3 respectively. Rutherford scattering cross sections were assumed for the RBS analysis and NRA data were analysed using the scattering cross sections of Möller and Besenbacher.[20] In order to avoid over-parameterisation, model composition profiles were restricted to either two or three layers, for which the composition and thickness was allowed to vary to obtain the best possible fit to the experimental data. Further particulars of data analysis with DataFurnace are discussed elsewhere.[21-23]

Neutron reflectometry.

Vertical concentration profiles of components within the spin-cast films were also determined by the neutron reflectometry (NR) analysis techniques using SURF at the science and technology facilities council (STFC) facility ISIS. Sample preparation was similar for NRA experiments, except that films were somewhat thinner (70 nm) in order to maximise the sensitivity of the measurement to changes in film thickness from the Kiessig fringes in the reflectivity profiles. NR offers significantly better depth

resolution (0.5 nm) than is achievable with IBA, provides a direct measure of film surface roughness and can be performed under atmospheric conditions. Specular reflectivity, R(Q), was measured from before the critical edge (Q ~ 0.01 Å^{-1} to the point at which the signal is indistinguishable from the background (Q~0.25 Å^{-1}). This measurement required three angles of incidence and approximately 2 hours of acquisition time per sample in order to obtain data of sufficient statistical quality over the entire Q-range. This latter factor imposes a requirement that films must be stable for at several hours, as any alteration in film thickness during measurement would make accurate interpretation of the data impossible.

The scattering length densities of the silicon substrate the organic components in the film are shown in Table 1, along with the approximate value for the native oxide layer, which is consistent with results that have been inferred from previous experiments on silicon substrates. [24-26]

RESULTS

Composition versus depth profiles for individual components within PVA films, which have been derived from ion beam analysis and neutron reflectometry experiments. For each composition profile presented, the numerical values for the layer composition and thickness are tabulated and have been provided as supporting information. (S.I.1.)

Table 1. List of scattering length densities for hydrogenous and deuterated materials

component	SLD x10^{6} / Å^{-2}
PVA	0.67
Si	2.07
SiO_x	3.0-3.5
glycerol	0.61
d_5-glycerol	4.65
$C_{12}E_5$	0.13
d_{25}-$C_{12}E_5$	4.47

Segregation of individual components in PVA films

Nuclear reaction analysis data and fits for d-glycerol in PVA films are shown along with the derived concentration profiles for these mixtures in figure 1a. This technique allows the depth distribution of a single deuterium labelled species to be isolated from an arbitrary matrix of other components over a range which can be chosen to be between approximately 100 nm to 10 μm, and with a depth resolution of around 5-10% of the range. The sharp onset in the spectrum at channel 12.77 MeV corresponds to deuterated species present at the film surface, and the gradual decline in proton yield (counts per channel) is in this case due to the decrease in nuclear reaction scattering cross-section as the beam penetrates the sample and loses energy. Due to the inverse kinematics of the nuclear reaction in backscattering geometry, protons generated at the surface of the sample are detected at the lowest energy and protons from greater depths are detected at higher energies.[27] The curve fitted to the experimental data is the calculated proton yield for a homogeneous distribution of d_5-glycerol, as indicated by the flat composition versus depth profile. Note that ion beam analysis is sensitive to composition in terms of 'atom' fraction, where molecules are represented by 'atoms' of their average elemental composition. (The mass fractions of the components would be scaled by their relative densities.) The small discrepancy between the model fit and the experimental data at approximately 13.1 MeV indicates some roughness or variation in effective film thickness, which is not accounted for in the model composition profile. Nevertheless, the data are consistent with the d_5-glycerol being evenly vertically distributed within the film. Figure 1b shows complementary NR data for the even distribution of plasticizer throughout the matrix. Although the film studied in this experiment was somewhat thinner and contains a lower loading of d_5-glycerol than the sample examined by NRA, the result is qualitatively similar; i.e. the d_5-glycerol is evenly distributed throughout the depth of the film.

In complete contrast to the behaviour observed for d5-glycerol, Figure 2a shows that the non-ionic surfactant d_{25}-$C_{12}E_5$ is very unevenly distributed within the PVA film. The large peak in counts per channel near 12.77 MeV corresponds to a significant surface excess of the surfactant, where surface excess is defined as

$$z^* = \int_0^\infty \varphi(z) - \varphi_b dz \quad (1)$$

Here, ϕ_b is the bulk concentration adjacent to the surface excess region, and $\phi(z)$ is the depth (z) dependent volume fraction profile of the near surface region. The fit to the experimental data yields the composition profile shown in the inset, from which z^* may be calculated. NR data presented in figure 2b, confirms the presence of surface and interfacial excesses of d_{25}-$C_{12}E_5$ in PVA, which forms spontaneously during spin-casting and is stable for at least the duration of the measurement. Furthermore,

NR is able to resolve the precise composition profile of the surface and interfacial region, and indicates that the surface and interfacial excess layers are typically not pure surfactant, but contain a significant amount of PVA too.

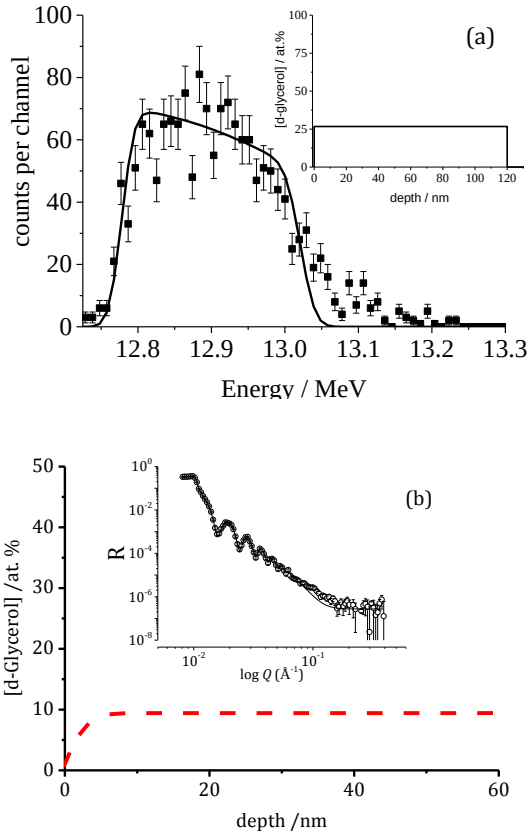

Figure 1(a). Nuclear reaction analysis data (proton spectrum) for 30% d-glycerol in thin PVA films. The fitted curve to the data corresponds to the composition versus depth profile of the d-glycerol, presented in the inset. (b) Neutron reflectometry data and fit and corresponding composition profile for 10% d-glycerol in thin PVA films.

The depth distribution of a cationic surfactant, CTAB, in PVA film is revealed by RBS results shown in figure 3. The solid curve fitted to the data data in the inset corresponds to the concentration profile of the main figure. In this case the scattering observed in the region of channels below 0.6 MeV is due to the lighter elements in the sample: C, O and Si, of which Si makes the dominant contribution. Scattering observed from 0.7-1.3 MeV arises from the Br- ions in the CTAB surfactant.

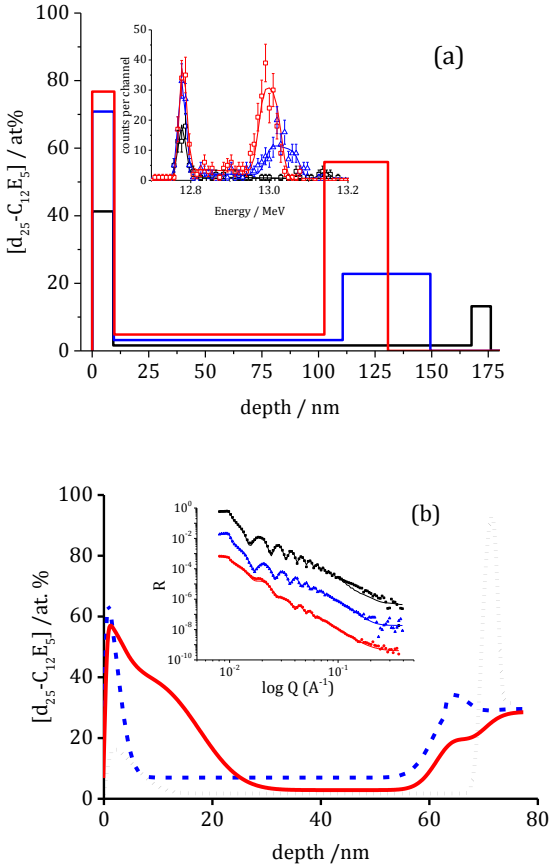

Figure 2(a). Nuclear reaction analysis data and Datafurnace fits for 5% (filled squares), 15% (open triangles) and 25% (filled circles) d_{25}-$C_{12}E_5$ in thin PVA films. The derived concentration profiles are shown in the inset. (b) Neutron reflectometry data (offset) and fits for 10% (filled squares), 20% (filled triangles) and 30% (filled circles) d_{25}-$C_{12}E_5$ in thin PVA films. The derived SLD profiles are shown in the inset.

The low energy edge of the RBS spectrum corresponding to Br around channel 100 is noticeably more diffuse than the high energy edge for surface Br. Some evidence for film roughness was apparent from the relatively diffuse tail in the RBS spectrum around 0.8 MeV, and 0.55 MeV, which correspond to the elemental composition profiles of the deepest Br and Si closest to the film surface respectively. By fitting a film roughness of 10% of the total film thickness,[28] both of these features are captured by the

DataFurnace fit to the experimental data. Most significantly, the CTAB in PVA is remarkably evenly distributed throughout the 187 nm film. There is no evidence for surface segregation, which would be apparent as a sharp peak around channel 1.3 MeV. The calculated surfactant concentration obtainable from Figure 3 is 25% which is in good agreement with the nominal composition of the spin-cast film.

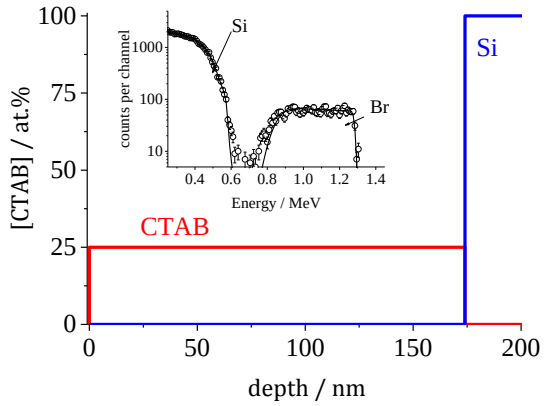

Figure 3. Depth distribution of CTAB in thin, spin-cast PVA film. The inset shows the RBS data and fits for thin films from which the profile was determined.

Influence of glycerol plasticiser on d_{25}-$C_{12}E_5$ non-ionic surfactant

Despite the d_5-glycerol plasticizer showing no inherent surface segregation itself, the presence of glycerol in the PVA film has quite a profound and unexpected impact on the distribution of the surfactants. Figure 4 shows NRA data and fits for the influence of (hydrogenous) glycerol on the depth distribution of d_{25}-$C_{12}E_5$ in PVA. The mass fraction of surfactant was maintained at 30% and the mass fraction of glycerol was systematically increased by replacing some of the PVA in the film with glycerol. With increasing glycerol concentration, the surface activity of the non-ionic surfactant systematically decreases. This is evident from the reduction in the relative size of the surface excess peak at ~12.77 MeV in the NRA data when compared to the protons detected at higher energies corresponding to d_{25}-$C_{12}E_5$ that is deeper within the PVA film. The model composition profiles determined from fits to the NRA data enable this effect to be quantified. Using neutron reflectometry, the influence of glycerol on the nature of the surface excess profile was investigated. As well as confirming the result obtained by NRA, the near-surface composition profiles presented in figure 5, show that the primary influence of glycerol is on the surface concentration, rather than the spatial extent of the surface enriched layer. Furthermore, the high sensitivity of NR was able to show that when the isotopic labelling was reversed, it was evident that the d5-glycerol was enriched at the surface of $C_{12}E_5$ + PVA films.

While it is clear that glycerol has the effect of reducing the surface activity of $C_{12}E_5$, it appears that the same plasticiser has the opposite influence over the distribution of CTAB. Here, the addition of glycerol to the PVA induces a dramatic change in the RBS spectra with significant peaks emerging in the parts of the spectra corresponding to surface and interfacial bromide. The roughness was only marginally greater than was observed for the glycerol free film with values of 11-16 nm being determined from the RBS analysis. In other words, we demonstrate significant levels of both surface and interfacial activity in the CTAB, when glycerol is added to the formulation, despite neither CTAB nor d-glycerol showing any discernible segregation when present in isolation in PVA. So far the effect of plasticiser on surfactant has been studied; a secondary experiment was carried out with NR to determine the effect of surfactant on plasticiser distribution. The same result in binary films of d-glycerol and PVA was found; in the absence of surfactant, d-glycerol shows no surface activity. However upon introduction of h-$C_{12}E_5$ to the system, which is similar in SLD to the PVA matrix, leaving d-glycerol as the only labelled species, the concentration profile of d-glycerol takes a form, which is remarkably similar to that of the non-ionic surfactant. (figure 5(b)).

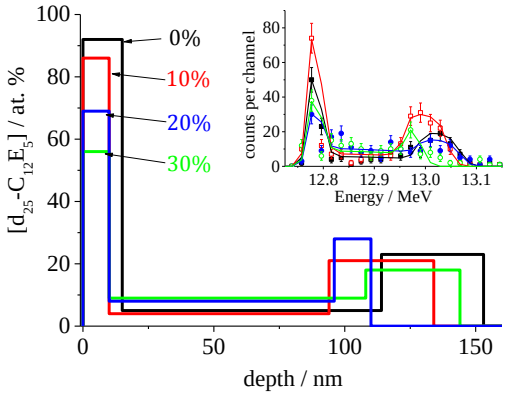

Figure 4. Concentration profiles of 30% d_{25}-$C_{12}E_5$ in mixed PVA/glycerol films as a function of glycerol content. Glycerol concentrations are annotated in the main figure. NRA data and fits are shown in the inset.

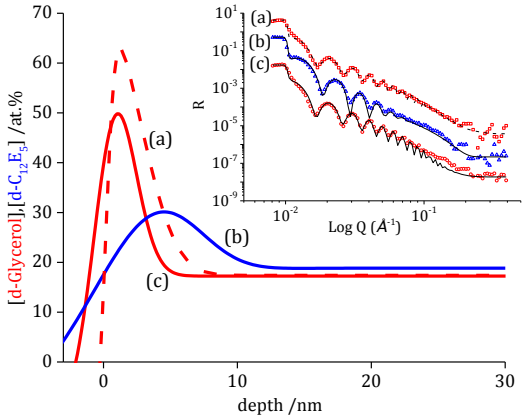

Figure 5. NR data, fits and composition profiles for (a) 20% d_{25}-$C_{12}E_5$ in PVA, (b) 20% d5-glycerol and 20% $C_{12}E_5$ in PVA and (c) 20% d_{25}-$C_{12}E_5$ and 20% glycerol in PVA. The composition profiles are for the single deuterated component in each case.

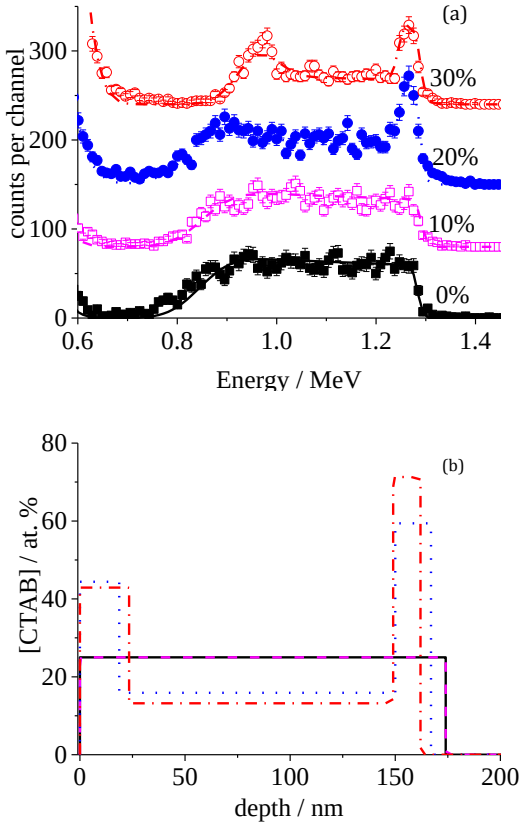

Figure 6(a). RBS data and fits for the depth distribution of 25% CTAB in mixed PVA/glycerol films as a function of glycerol content. Data are offset for clarity and annotated with glycerol content. (b) Concentration profiles corresponding to the Datafurnace fits: black (0%), mauve (10%), blue (20%), red (30%).

DISCUSSION

Surface enrichment in two-component PVA films

It is well documented[29-30] that glycerol is sufficiently compatible with PVA to be an effective plasticiser, and our results are also consistent with a single phase mixture in that the depth distribution is at least vertically homogeneous. Surface adsorption on the other hand is the defining feature of surfactants; furthermore blooming of plasticisers to surfaces is also is well known for many materials. Therefore, some level of surface enrichment of these molecules at the surface of PVA film might still be expected. In the following discussion we address some of the underlying physical causes of surface segregation in order to evaluate their contributions to the observed behaviour.

In these mixtures of relatively large (PVA) and smaller (glycerol or surfactant) molecules, there is a configurational entropy penalty associated with deformation of larger molecules at a planar surface; therefore some surface and interfacial segregation of the smaller molecules might be expected. However, this is a relatively weak effect and in single phase mixtures the levels of surface adsorption are limited to partial coverage[10] and have a correlation length τ, which is given by

$$\frac{1}{\tau^2} = \frac{\phi_2}{R_1^2} + \frac{\phi_1}{R_2^2} \qquad (2)$$

where ϕ_i is the bulk volume fraction of the i^{th} component and R_i is the characteristic dimension of this component.[31] From the data of Brandrup and Immergut[32] we obtain the expression for the radius of gyration of PVA as

$$R_g/nm = 0.0388 M_w^{\frac{1}{2}} \qquad (3)$$

where M_w is the molecular weight in g/mol, yielding a value of approximately 6.7 – 10.5 nm for the PVA used in this work. Because the d-glycerol has a R_g of approximately 0.5 nm, the correlation length of any adsorbed layer with 30% d-glycerol in PVA would be dominated by this smaller component and τ would be of the order of 0.6 nm. This value is very small compared to the depth resolution of NRA. While we cannot exclude the possibility of some enrichment of d-glycerol at PVA

surfaces our NRA results at least confirm that the plasticised film is behaving as a single phase mixture.

The concentration profiles of CTAB in PVA were qualitatively identical to glycerol, which is much more surprising. Firstly, the RBS measurement is more sensitive than NRA because of the strong sensitivity of Rutherford backscattering to heavy elements such as bromine, especially at the surface of a film of light elements. We can predict that even a partial monolayer of CTAB would fall within the detection threshold of the measurement, and this is demonstrated in a quantitative simulation provided in the supporting information (S.I.2). Moreover, as a surfactant CTAB, might be expected to display some surface or interfacial activity. Our results appear to suggest that the propensity of small molecules to segregate the surface is overwhelmed by some more significant factor. We therefore turn our attention to the surface energies of the components present in the films.

PVA surface energy has been shown to vary with DH and M_w. [33] Two sources quote the surface energy of PVA as 37 mN/m at 20 °C [34-35] but values of 42-59 mN/m have been given by others.[36-38] The surface energy of PVA decreases with decreasing DH and M_w, and since the PVA used in this study is classed as 'partially hydrolysed' (contains at least 10% PVAc) the surface energy is likely to be at the lower end of the range of values established by other authors. In comparison, glycerol has a surface tension value of 63.4 mN/m at 20 °C,[39] much higher than the surface of PVA. In this case, adsorption would not cause any reduction in surface energy, so is not expected to be spontaneous.

While there is considerable variation of energy values for PVA in the literature, all are much lower than the surface tension of water. If CTAB adsorption does not significantly reduce the surface energy of the PVA film in which it is dispersed, then there would be little thermodynamic impetus for this process to occur spontaneously. We are unaware of any measure of the surface energy of CTAB in the pure state, and the relevance of such a measure on an ionic solid to the dispersed and dissociated surfactant in PVA is questionable. However, CTAB surface activity has been rigorously studied in aqueous solutions, where this surfactant can reduce the surface tension from 72 mN/m to a limiting surface tension (at concentrations above the critical micelle concentration, c.m.c.) of 32-36 mN/m.[40] The lower values were obtained when KCl was added to the solution, which has the effect of screening the charged groups of the surfactant, enabling closer CTAB packing on the solution surface. In our case, no such additional ions are present, so while we should be cautious in comparing the surface energy of PVA to that of a CTAB solution above the c.m.c., it is plausible that the lack of adsorption of CTAB at the PVA-air surface is due to their relatively similar surface energies.

In contrast to the plasticiser and cationic surfactant, our NRA and NR experiments show clear surface segregation of the non-ionic surfactant d_{25}-$C_{12}E_5$ to the surface of PVA films. A powerful feature of NRA is that it allows the surface excess of the surfactant to be determined directly, and it appears that there is a layer of ~8 nm of almost pure deuterated surfactant at the air surface. The magnitude of surface excess is very significant, since it far exceeds the maximum value obtainable for a dense monolayer of the surfactant. The maximum all-trans length of a $C_{12}E_5$ molecule is ~3.7 nm, and this defines the limiting value of adsorbed layer thickness that could exist if the surfactant molecules were orientated perpendicular to the film surface. Since the measured surface excess is approximately twice this value, it accounts for the equivalent of approximately 2 end-to-end molecules. Both experimental and computational studies of $C_{12}E_5$ adsorption on water indicate that it forms single layers with the hydrophobic tails outermost and somewhat tilted with respect to the sample normal.[15, 41] Although NRA lacks the resolution required to characterise the orientation of the d_{25}-$C_{12}E_5$ chains, it does unambiguously reveal the presence of multilayer adsorption at the surface, which signifies the presence of a wetting layer of surfactant coexisting with the PVA-rich film beneath it.

Surface tension and surface energy arguments can again help to rationalise this phenomenon; $C_{12}E_5$ has a limiting surface tension of 29.9 mN/m at concentrations ≥ 0.1 mM in water[42], which is appreciably lower than the equivalent measure of any other component under consideration. It therefore seems likely that surface adsorption of d_{25}-$C_{12}E_5$ in PVA is favoured by the reduction in surface energy associated with this process, and is considerably enhanced by the relatively poor compatibility of these materials. Inspection of the composition profiles in figure 2 suggests that the maximum concentration of d_{25}-$C_{12}E_5$ in PVA in the bulk of the film is approximately 10%, which could be taken as an upper limit to the binodal composition of the mixture.

Influence of plasticiser on surface properties of 3 component PVA films.

In order to resolve the origin of the large surface excess of d_{25}-$C_{12}E_5$ in PVA films, the impact of replacing some fraction of the PVA with (hydrogenous) glycerol was explored. Both the NRA and the NR experiments in figures 4 and 5 respectively clearly showed that when some of the PVA in the film is replaced with glycerol, there is a fairly systematic decrease in the surface excess of d_{25}-$C_{12}E_5$. The surface excess values calculated from the NRA experiments, in which the bulk composition of the film is taken to be the composition of the middle region adjacent to the surface excess, is presented in figure 7. This decrease cannot be explained if the driving force for d_{25}-$C_{12}E_5$ surface adsorption were purely due to the difference in surface tension. We can draw this conclusion because glycerol has a higher surface tension than any of the reported surface energy values for PVA. On this basis, it is evident that the surface segregation seen for d_{25}-$C_{12}E_5$ in PVA and PVA/glycerol mixtures may be directed by differences in surface energy, but the

extent of segregation arises largely from the incompatibility between the surfactant and the other components. Furthermore, it appears that glycerol leads to an increase in compatibility of d_{25}-$C_{12}E_5$ with the matrix; increasing the solubility of the surfactant and so decreasing the proportion of surfactant that segregates to the film surface.

The relatively high compatibility of d_{25}-$C_{12}E_5$ in glycerol is further supported by the evidence of the NR experiment in which the glycerol was the only labelled component (figure 5). In this case, the contrast in SLD between the PVA and the $C_{12}E_5$ is nearly an order of magnitude smaller than the contrast between the d_5-glycerol and these components; therefore the NR signal is completely dominated by the depth distribution of the plasticiser. In the absence of $C_{12}E_5$, d_5-glycerol was shown to have no surface activity in PVA film (figure 1), but it is clear from figure 5 that it becomes surface-active when $C_{12}E_5$ is also present. We can therefore conclude that the compatibility between $C_{12}E_5$ and glycerol causes them to become co-located; the $C_{12}E_5$ induces some surface segregation of the glycerol, and the glycerol, being relatively compatible with PVA also, enables more $C_{12}E_5$ to be distributed throughout the bulk of the PVA film.

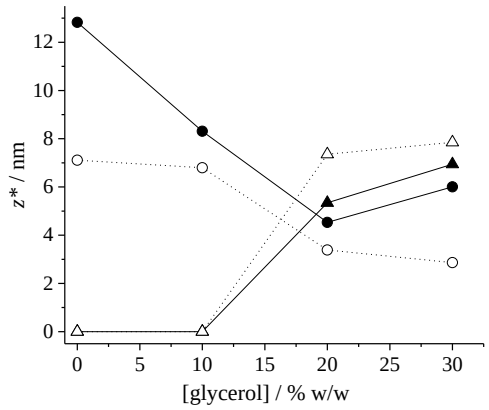

Figure 7. Surface excess (solid symbols and solid lines) and interfacial excess (open symbols and dotted lines) of d_{25}-$C_{12}E_5$ (circles) and CTAB (triangles) in PVA film as a function of added glycerol concentration.

Given the tendency of glycerol to suppress the surface segregation of d_{25}-$C_{12}E_5$ in PVA, the increase in surface and interfacial activity of CTAB in PVA with increasing glycerol content, which is apparent from the appearance of the peaks in the RBS data in figure 6, is quite surprising. The surface and interfacial excess values derived from the composition profiles are shown in figure 7. The surface activity of CTAB will depend on surface tension of the medium in which it is dispersed. In this case the medium is a mixture of PVA and glycerol, for which the surface tension would be dominated by that of the lower surface tension component, PVA. Increasing the amount of glycerol in the PVA should not significantly increase the surface tension of the mixture; therefore it is unlikely to drive the dramatic dependence of surface activity on glycerol content. It is most likely that CTAB is much less compatible with PVA when it is plasticised with glycerol than when it is in its pure state. The reason for this is still not clear, but we speculate that glycerol out-competes CTAB for its favourable interaction with amorphous regions of PVA. Although beyond the scope of this first investigation, it seems plausible that CTAB cations bind to the lone pairs of PVA hydroxyl groups in a similar manner to the behaviour that have been previously reported for film forming mixtures of CTAB and imine groups of PEI.[14] It would be interesting to explore whether similar mesostructures such as cylindrical micelles are formed between CTAB and PVA, as these might considerable reduce the mobility of CTAB and so inhibit the surface segregation in unplasticised films.

An interesting consequence of the diametrically opposed changes in surfactant solubility in PVA as a function of plasticiser content is that the barrier properties of this film with respect to different surfactants may also follow this pattern; i.e. unplasticised PVA may be a relatively good barrier with respect to non-ionic surfactants like $C_{12}E_5$ and while plasticised PVA may be a better barrier with respect to cationic surfactants.

Interfacial segregation of surfactants

Our discussion has so far focused on the segregation of surfactants at the exposed surfaces of PVA films in the presence or absence of plasticiser, but it is noticeable that in many cases the surfactant species was also found to be enriched at the buried interface between the film and the siliconoxide surface of the silicon wafer substrate. The magnitude of the excess of surfactant at the siliconoxide interface is comparable to that of the surface excess, although perhaps having a more diffuse distribution. These values are compared in figure 7. This phenomenon has some significance to our interpretation of our results, since it further supports the case for surface and interfacial segregation being driven by incompatibility, leading to phase-separated wetting layers on the film surface. The observed concentration profiles are consistent with the profiles seen for surface directed spinodal decomposition in

polymer blends by several authors in the 1990s.[12, 43-45] Formation of wetting layers on silica is perhaps also significant in the context of some application where silica particles may be added to PVA films to prevent cohesion between PVA surfaces. Our results indicate that some combinations of plasticiser and surfactant in PVA could lead to the silica particles becoming engulfed by the surfactant and may reduce their effectiveness in this application.

CONCLUSIONS

We have explored the surface and interfacial segregation behaviour of two surfactants and one plasticiser in PVA film by a variety of ion beam analysis techniques and neutron reflectometry, which allow the surface excess of individual components to be isolated from these mixtures. In binary mixtures with PVA, neither the model plasticiser (d-glycerol) nor a cationic surfactant (CTAB) showed any discernible surface segregation within the detection limit of the measurements. However, d_{25}-$C_{12}E_5$ was found to be strongly segregated to the exposed (air) surface of PVA films and the surface excess was quantified by NRA. It appears that the surface segregation is directed by surface energy differences, but augmented by the incompatibility of the surfactants with the matrix in which they are dispersed. The presence or absence of surface segregation is therefore consistent with the relatively low limiting surface tension of $C_{12}E_5$ solutions, somewhat higher limiting surface tension of CTAB and significantly higher surface tension of glycerol. The addition of glycerol plasticiser to the PVA + surfactant mixed films has some dramatic and unexpected effects: the surface activity of d_{25}-$C_{12}E_5$ systematically decreases with increasing glycerol content, while the opposite effect was observed when glycerol was included in the PVA + CTAB films. We attribute these effects to the different compatibility of these surfactants with respect to glycerol and the surface segregation being driven significantly by incompatibility. These opposing trends with respect to plasticiser content has significant implications for the barrier properties of plasticised PVA films with respect to surfactant mixtures, as well as the application of inorganic nanoparticles on PVA films to inhibit cohesion.

ACKNOWLEDGEMENTS: We are grateful to EPSRC / Procter and Gamble (UK) for supporting this project as an industrial CASE award EP/L505419/1. We are also grateful to STFC for provision of the neutron reflection facilities.

REFERENCES

1. Tripathi, S.; Mehrotra, G. K.; Dutta, P. K., Physicochemical and bioactivity of cross-linked chitosan–PVA film for food packaging applications. *Int. J. Bio. Macromols.* **2009,** *45*, 372-376.

2. Chaouat, M.; Le Visage, C.; Baille, W. E.; Escoubet, B.; Chaubet, F.; Mateescu, M. A.; Letourneur, D., A Novel Cross-linked Poly(vinyl alcohol) (PVA) for Vascular Grafts. *Adv. Funct. Mater.* **2008,** (18), 2855-2861.

3. Ma, R.; Xiong, D.; Miao, F.; Zhang, J.; Peng, Y., Novel PVP/PVA hydrogels for articular cartilage replacement. *Mater. Sci. Eng., C* **2009,** *29* (6), 1979-1983.

4. Winterton, L. C.; Lally, J. M.; Sentell, K. B.; Chapoy, L. L., The elution of poly (vinyl alcohol) from a contact lens: The realization of a time release moisturizing agent/artificial tear. *Journal of Biomedical Materials Research Part B: Applied Biomaterials* **2007,** *80B* (2), 424-432.

5. Poole, T. R. G.; Gillespie, I. H.; Knee, G.; Whitworth, J., Microscopic fragmentation of ophthalmic surgical sponge spears used for delivery of antiproliferative agents in glaucoma filtering surgery. *Br. J. Ophthalmol.* **2002,** *12* (86), 1448-1449.

6. Hassan, C. M.; Peppas, N. A., Structure and Applications of Poly(vinyl alcohol) Hydrogels Produced by Conventional Crosslinking or by Freezing/Thawing Methods. In *Biopolymers · PVA Hydrogels, Anionic Polymerisation Nanocomposites*, Springer Berlin Heidelberg: 2000; Vol. 153, pp 37-65.

7. Moukwa, M.; Youn, D.; Hassanali, M., Effects of degree of polymerization of water soluble polymers on concrete properties. *Cem. Concr. Res.* **1993,** *23*, 122-130.

8. Termonia, Y.; Meakin, P.; Smith, P., Theoretical study of the influence of the molecular weight on the maximum tensile strength of polymer fibers. *Macromolecules* **1985,** *18* (11), 2246-2252.

9. Mohsin, M.; Hossin, A.; Haik, Y., Thermal and mechanical properties of poly(vinyl alcohol) plasticized with glycerol. *J. Appl. Polym. Sci.* **2011,** *122* (5), 3102-3109.

10. Hariharan, A.; Kumar, S. K.; Russell, T. P., Reversal of the Isotopic Effect in the Surface Behavior of Binary Polymer Blends. *J. Chem. Phys.* **1993,** *98* (5), 4163-4173.

11. Hunter, R. J., *Foundations of Colloid Science*. Clarendon Press: Oxford, 1987; Vol. 1.

12. Geoghegan, M.; Jones, R. A. L.; Clough, A. S., Surface directed spinodal decomposition in a partially miscible polymer blend. *J. Chem. Phys.* **1995,** *103* (7), 2719-24.

13. Campbell, R. A.; Edler, K. J., Growth-collapse mechanism of PEI-CTAB films at the air-water interface. *Soft Matter* **2011,** *7* (23), 11125-11132.

14. Edler, K. J.; Wasbrough, M. J.; Holdaway, J. A.; O'Driscoll, B. M. D., Self-Assembled Films Formed at the Air-Water Interface from CTAB/SDS Mixtures with Water-Soluble Polymers. *Langmuir* **2009,** *25* (7), 4047-4055.

15. Lu, J. R.; Li, Z. X.; Thomas, R. K.; Binks, B. P.; Crichton, D.; Fletcher, P. D. I.; McNab, J. R.; Penfold, J., The Structure of Monododecyl Pentaethylene Glycol Monolayers with and without Added Dodecane at the Air/Solution Interface: A Neutron Reflection Study. *J. Phys. Chem. B.* **1998,** *102* (30), 5785-5793.

16. Lu, J. R.; Hromadova, M.; Thomas, R. K.; Penfold, J., Neutron reflection from triethylene glycol monododecyl ether adsorbed at the air-liquid interface: the variation of the hydrocarbon chain distribution with surface concentration. *Langmuir* **1993,** *9* (9), 2417-2425.

17. Thompson, R. L., Surface and Interfacial Characterization: Ion Beam Analysis. In *Polymer Science: A*

Comprehensive Reference, Moeller, M.; Matyjaszewski, K., Eds. Elsevier BV: Amsterdam, 2012; Vol. 2, pp 661-681.

18. Composto, R. J.; Walters, R. M.; Genzer, J., Application of Ion Scattering Techniques to Characterise Polymer Surfaces and Interfaces. *Materials Science and Engineering R* **2002,** *R38* (3-4), 107-180.

19. Barradas, N. P.; Jeynes, C.; Webb, R. P., Simulated annealing analysis of Rutherford backscattering data. *Applied Physics Letters* **1997,** *71* (2), 291-293.

20. Möller, W.; Besenbacher, F., Note on the He-3+D Nuclear-Reaction Cross-Section. *Nucl. Instrum. Methods* **1980,** *168* (1-3), 111-114.

21. Jeynes, C.; Barradas, N. P.; Szilágyi, E., Accurate Determination of Quantity of Material in Thin Films by Rutherford Backscattering Spectrometry. *Anal. Chem.* **2012,** *84* (14), 6061-6069.

22. Jeynes, C.; Bailey, M. J.; Bright, N. J.; Christopher, M. E.; Grime, G. W.; Jones, B. N.; Palitsin, V. V.; Webb, R. P., "Total IBA" - Where are we? *Nucl. Instrum. Methods Phys. Res. Sect. B-Beam Interact. Mater. Atoms* **2012,** *271*, 107-118.

23. Barradas, N. P.; Jeynes, C., Advanced physics and algorithms in the IBA DataFurnace. *Nucl. Instrum. Methods Phys. Res., Sect. B* **2008,** *266* (8), 1875-1879.

24. Bucknall, D. G.; Butler, S. A.; Higgins, J. S., Studying polymer interfaces using neutron reflection. In *Scattering from Polymers*, 2000; Vol. 739, pp 57-73.

25. James, C. D.; Jeynes, C.; Barradas, N. P.; Clifton, L.; Dalgliesh, R. M.; Smith, R. F.; Sankey, S. W.; Hutchings, L. R.; Thompson, R. L., Modifying Polyester Surfaces with Incompatible Polymer Additives. *React. Funct. Polym.* **2015,** *89*, 40-48.

26. Hardman, S. J.; Hutchings, L. R.; Clarke, N.; Kimani, S. M.; Mears, L. L. E.; Smith, E. F.; Webster, J. R. P.; Thompson, R. L., Surface Modification of Polyethylene with Multi-End-Functional Polyethylene Additives. *Langmuir* **2012,** *28* (11), 5125-5137.

27. Payne, R. S.; Clough, A. S.; Murphy, P.; Mills, P. J., Use of the D(He-3,P)He-4 Reaction to Study Polymer Diffusion in Polymer Melts. *Nucl. Instrum. Methods Phys. Res., Sect. B* **1989,** *42* (1), 130-134.

28. Barradas, N. P., Rutherford backscattering analysis of thin films and superlattices with roughness. *J. Phys. D-Appl. Phys.* **2001,** *34* (14), 2109-2116.

29. Su, J.-F.; Huang, Z.; Liu, K.; Fu, L.-L.; Liu, H.-R., Mechanical Properties, Biodegradation and Water Vapor Permeability of Blend Films of Soy Protein Isolate and Poly (vinyl alcohol) Compatibilized by Glycerol. *Polym. Bull.* **2007,** *58* (5-6), 913-921.

30. Sakellariou, P.; Hassan, A.; Rowe, R. C., Plasticization of aqueous poly(vinyl alcohol) and hydroxypropyl methylcellulose with polyethylene glycols and glycerol. *Eur. Polym. J.* **1993,** *29* (7), 937-943.

31. Hariharan, A.; Kumar, S. K.; Russell, T. P., A lattice model for the surface segregation of polymer chains due to molecular weight effects. *Macromolecules* **1990,** *23* (15), 3584-3592.

32. Brandrup, J.; Immergut, E. H., *Polymer Handbook*. 3rd ed.; Wiley: New York, 1989.

33. Marten, F. L., Vinyl Alcohol Polymers. In *Kirk-Othmer Encyclopedia of Chemical Technology*, John Wiley & Sons, Inc.: 2000.

34. Polmanteer, K. E., Current perspectives on silicone rubber technology. *Rubber Chem. and Tech.* **1981,** *54* (5), 1051-1080.

35. Wu, S., Estimation of the critical surface tension for polymers from molecular constitution by a modified Hildebrand-Scott equation. *J. Phys. Chem.* **1968,** *72*, 3332.

36. Lee, L. H., Relationships between surface wettability and glass temperatures of high polymers. *J. Appl. Polym. Sci.* **1968,** *12*, 719.

37. Van Krevelen, D. W.; Hoftyzer, P. J., Elsevier, New York, N.Y.: 1976.

38. van Oss, C. J.; Chaudhury, M. K.; Good, R. J., Monopolar surfaces. *Advances in Colloid and Interface Science* **1987,** *28*, 35-64.

39. Takamura, K.; Fischer, H.; Morrow, N. R., Physical properties of aqueous glycerol solutions. *Journal of Petroleum Science and Engineering* **2012,** *98–99*, 50-60.

40. Adamczyk, Z.; Para, G.; Warszyński, P., Influence of Ionic Strength on Surface Tension of Cetyltrimethylammonium Bromide. *Langmuir* **1999,** *15* (24), 8383-8387.

41. Cuny, V.; Antoni, M.; Arbelot, M.; Liggieri, L., Structural properties and dynamics of C12E5 molecules adsorbed at water/air interfaces: A molecular dynamic study. *Colloids Surf., A* **2008,** *323* (1–3), 180-191.

42. Kjellin, U. R. M.; Claesson, P. M.; Linse, P., Surface Properties of Tetra(ethylene oxide) Dodecyl Amide Compared with Poly(ethylene oxide) Surfactants. 1. Effect of the Headgroup on Adsorption. *Langmuir* **2002,** *18* (18), 6745-6753.

43. Jones, R. A. L.; Norton, L. J.; Kramer, E. J.; Bates, F. S.; Wiltzius, P., Surface-directed spinodal decomposition. *Phys. Rev. Lett.* **1991,** *66* (10), 1326-9.

44. Bruder, F.; Brenn, R., Spinodal Decomposition in Thin-Films of a Polymer Blend. *Phys. Rev. Lett.* **1992,** *69* (4), 624-627.

45. Krausch, G.; Dai, C. A.; Kramer, E. J.; Marko, J. F.; Bates, F. S., Interference of Spinodal Waves in Thin Polymer-Films. *Macromolecules* **1993,** *26* (21), 5566-5571.

SYNOPSIS TOC :

Surface and interfacial activity of surfactants in PVA film is controlled by their surface energies and their compatibility with PVA and glycerol plasticizer.